

ANALYSIS OF TF-SF BOUNDARY FOR 2D-FDTD WITH PLANE P -WAVE PROPAGATION IN LAYERED DISPERSIVE AND LOSSY MEDIA

Y.-N. Jiang, D.-B. Ge, and S.-J. Ding

Department of Physics, School of Science
Xidian University
Xi'an 710071, China

Abstract—In the application of two-dimension (2D) finite-difference time-domain (FDTD) to scattering analysis of object embedded in layered media, the incident electromagnetic wave propagation is much more complicated, it can not inject the plane wave source by traditional method. To solve this problem, the Π -shape total-field/scattering-field (TF-SF) boundary scheme is presented. The side TF-SF boundaries are governed by the modified 1D Maxwell's equations, but the discretization for which to p -wave is more difficult than n -wave. Then an auxiliary magnetic variable is used, which can develop the modified 1D-FDTD to p -wave without any approximately. To truncate the modified 1D-FDTD, the *convolutional* perfectly matched layer (CPML) absorbing boundary condition (ABC) is also given. Examples show the feasibility and applicability of proposed Π -shape TF/SF boundaries scheme.

1. INTRODUCTION

The analysis of scattering in layered media is the most popular research area, which includes the detection of a target in the subsurface or submarine, on the ground or water surface and in the low altitude, the checking of the biological body, the nondestructive examination of optical element and so on. The finite-difference time-domain (FDTD) method [1] is one of the most effective techniques for analyzing electromagnetic problems for complex target. However, being the reflection and transmission waves in dispersive layered media, the incident electromagnetic wave propagation becomes much more complicated, which causes difficulty in the plane wave source injection in layered media.

The three-wave method [2] was used to solve this problem currently, which needs to work out the reflection and transmission wave in frequency-domain at each interface, and transform them into time-domain by Fourier transform, then applied to the total-field/scattering-field (TF-SF) boundary. Yi et al. [3] presented a scheme of 2D-FDTD with an obliquely incident angle, which is available to the non-dispersive media. Based on [3], Winton et al. [4] derived the modified 1D Maxwell's equations for n -wave (TM-wave) and p -wave (TE-wave) obliquely incident to layered dispersive media. However the treatment of 1D-FDTD to p -wave is more difficult than to n -wave. The modified 1D-FDTD to n -wave can be discretised directly. However, the similar treatment for p -wave has to be restricted to the modulated pulse of narrow band, because the transmission angle is frequency dependent in dispersive media. The other method proposed by Capoglu et al. [5] using a magnetic auxiliary variable, but it is still restricted to the non-dispersion problem.

In this paper, the computation scheme suitable for layered dispersive and lossy media is presented in Section 2. In Section 3, the modified 1D Maxwell's equation to p -wave is developed in layered dispersive and lossy media. The *convolutional* perfectly matched layer (CPML) absorbing boundary condition (ABC) to modified 1D-FDTD is also given. And then the treatment of incident wave along upper and lower TF-SF boundaries is discussed. Three examples are presented in Section 4, which show the effectiveness of proposed method applicable to the obliquely incident plane wave in layered dispersive and lossy media. In Section 5, we conclude the study.

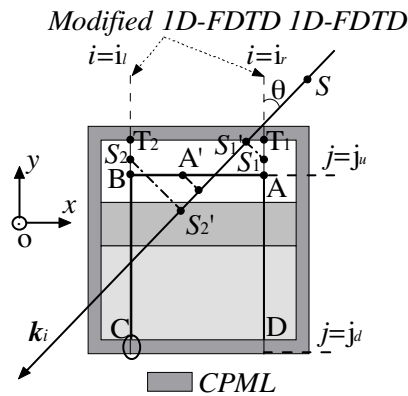


Figure 1. Geometry of Π -shape TF-SF boundary for layered dispersive and lossy media scattering problem.

2. CALCULATION SCHEME

The configuration of layered dispersive and lossy media is shown in Figure 1. The calculation scheme for the scattering problem is as follows: (1) A traditional 1D-FDTD is used to generate an obliquely incident wave in free space along \mathbf{k}_i direction, where S represents the point source in free space. (2) We use the modified 1D-FDTD to simulate the incident wave along side TF-SF boundary [4], viz. AD and BC , where S_1 and S_2 represent the point source in modified 1D-FDTD on AD and BC , respectively. Their projections onto \mathbf{k}_i direction are S'_1 and S'_2 , respectively. The incidence wave on S_1 and S_2 for modified 1D-FDTD can then be derived by linear interpolation to traditional 1D-FDTD [6–8]. This ensures the synchronization of incidence wave along the side TF-SF boundary AD and BC . (3) The upper TF-SF boundary AB is located in free space. The incident wave is in fact a duplication of the waveform at the corner A or B of TF-SF boundary with a proper time delay. (4) The lower TF-SF boundary can be treated by the same way as the upper TF-SF, if the lowest layer medium is non-dispersive and lossless. If the lowest layer medium is dispersive and lossy medium, we extend the side TF-SF downwards into CPML, as indicated by ellipse in Figure 1. It makes sure that the downward traveling wave is absorbed at lower media by CPML. This is an open TF-SF scheme with Π -shape that is not necessary to determine the incidence wave along the lower TF-SF as it does in the closed TF-SF scheme [6].

3. THEORY AND ANALYSIS

In the phasor domain, the relative permittivity of a single-pole Debye dispersive and lossy medium [6] is given by

$$\varepsilon_r(\omega) = \varepsilon_\infty + \frac{\Delta\varepsilon}{1 + j\omega\tau} + \frac{\sigma}{j\omega\varepsilon_0} \quad (1)$$

where ε_s is the static relative permittivity, ε_∞ is the infinite-frequency limit for the relative permittivity, they satisfy $\Delta\varepsilon = \varepsilon_s - \varepsilon_\infty$, τ is the single pole relaxation time, and σ is the conductivity.

The 2D-FDTD update equations to p -wave for electric and magnetic field with the grid spacing of Δx and Δy and the temporal

step of Δt are written as

$$H_z \Big|_{i,j}^{n+1} = CP(m) \cdot H_z \Big|_{i,j}^n - CQ(m) \cdot \left[\frac{E_y \Big|_{i+1/2,j}^{n+1/2} - E_y \Big|_{i-1/2,j}^{n+1/2}}{\Delta x} - \frac{E_x \Big|_{i+1/2,j}^{n+1/2} - E_x \Big|_{i-1/2,j}^{n+1/2}}{\Delta y} \right] \quad (2)$$

$$E_x \Big|_{i,j+1/2}^{n+1/2} = Ca(m) \cdot E_x \Big|_{i,j+1/2}^{n-1/2} + Cb(m) \cdot \frac{H_z \Big|_{i,j+1}^n - H_z \Big|_{i,j}^n}{\Delta y} - Cb(m) \cdot \frac{(1+k_d)}{2} J_{dx} \Big|_{i,j+1/2}^{n-1/2} \quad (3)$$

$$E_y \Big|_{i+1/2,j}^{n+1/2} = Ca(m) \cdot E_y \Big|_{i+1/2,j}^{n-1/2} - Cb(m) \cdot \frac{H_z \Big|_{i+1/2,j}^n - H_z \Big|_{i,j}^n}{\Delta x} - Cb(m) \cdot \frac{(1+k_d)}{2} J_{dy} \Big|_{i+1/2,j}^{n-1/2} \quad (4)$$

where J_d are the polarization current in time domain due to the Debye single pole. The subscripts i and j are the grid point along x and y direction, the superscript n is the number of time step. The coefficients in expressions (2)–(4) are listed as

$$Ca(m) = \frac{2\varepsilon_0\varepsilon_\infty + \beta_d - \sigma\Delta t}{2\varepsilon_0\varepsilon_\infty + \beta_d + \sigma\Delta t}; \quad \frac{2\Delta t}{2\varepsilon_0\varepsilon_\infty + \beta_d + \sigma\Delta t}; \quad k_d \frac{2\tau - \Delta t}{2\tau + \Delta t};$$

$$\beta_d = \frac{2\varepsilon_0\Delta\varepsilon t}{2\tau + \Delta t}; \quad CP(m) = \frac{2\mu_0 - \sigma_m\Delta t}{2\mu_0 + \sigma_m\Delta t}; \quad CQ(m) = \frac{2\Delta t}{2\mu_0 + \sigma_m\Delta t}$$

3.1. Treatment for Modified 1D Maxwell's Equation to p -wave

In Debye medium, the modified 1D Maxwell's equation to p -wave [4] in frequency domain can be expressed as

$$\frac{\partial H_{z1D}}{\partial y} = j\omega\varepsilon_0\varepsilon_r(y,\omega)E_{x1D}$$

$$\frac{k^2}{k_y^2} \frac{\partial E_{x1D}}{\partial y} = j\omega\mu_0 H_{z1D} \quad (5)$$

We consider the phase matching condition that the tangential component of the wave vector k_x is constant in each layer media. Where $k = \omega\sqrt{\mu_0\varepsilon_0\varepsilon_r}$, $k_{1x} = \omega\sqrt{\mu_0\varepsilon_0\varepsilon_{1r}}\sin\theta$ and $k_y^2 = k^2 - k_x^2 = k^2 - k_{1x}^2$, the Equation (5) can be rewritten as

$$\begin{aligned} \frac{\partial H_{z1D}}{\partial y} &= j\omega\varepsilon_0\varepsilon_r(y,\omega)E_{x1D} \\ \varepsilon_r(y,\omega)\frac{\partial E_{x1D}}{\partial y} &= j\omega\mu_0[\varepsilon_r(y,\omega) - \varepsilon_{1r}\sin^2\theta]H_{z1D} \end{aligned} \quad (6)$$

Note that $\varepsilon_r(\omega)$ is written as $\varepsilon_r(y,\omega)$ in Equation (6) to indicate the permittivity varies along y direction. In reference [4], an auxiliary variable $E'_{x1D} = \varepsilon_r(y,\omega)E_{x1D}$ is introduced to treat Equation (6). However, the left-hand of the second expression in (6) can not be substituted by partial derivative of E'_{x1D} with respect to y , because the relative permittivity of $\varepsilon_r(y,\omega)$ is the function of variable y . Winton may recognize this problem, he give an alternate TE_{1D} equations. But the alternate algorithm used the transmission angle at the center frequency of narrowband modulated pulse to instead the transmission angle to wideband. In dispersive media, this alternate algorithm is approximation; it can't be excited by the Gaussian's pulse with very wide band. To overcome this difficulty, we introduce a new auxiliary variable H'_{z1D} defined by

$$H'_{z1D} = \frac{[\varepsilon_r(y,\omega) - \varepsilon_{1r}\sin^2\theta]}{\varepsilon_r(y,\omega)}H_{z1D} \quad (7)$$

Equation (6) is then transformed into time domain and written as

$$\begin{aligned} \frac{\partial H_{z1D}}{\partial y} &= \varepsilon_0\varepsilon_\infty\frac{\partial E_{x1D}}{\partial t} + \sigma E_{x1D} + J_{x1D} \\ J_{x1D} + \tau\frac{\partial J_{x1D}}{\partial t} &= \varepsilon_0\Delta\varepsilon\frac{\partial E_{x1D}}{\partial t} \\ \frac{\partial E_{x1D}}{\partial y} &= \mu_0\frac{\partial H'_{z1D}}{\partial t} \end{aligned} \quad (8)$$

where J_{x1D} is the polarization current in time domain due to the Debye single pole.

To determine the relation of auxiliary variable H'_{z1D} with H_{z1D} in Equation (7), we let

$$\varepsilon'(y) = \varepsilon_\infty(y) - \varepsilon_{1r}\sin^2\theta \quad (9)$$

and substitute Equation (1) into Equation (7), then obtain

$$\left(\varepsilon_\infty + \frac{\Delta\varepsilon}{1 + j\omega\tau} + \frac{\sigma}{j\omega\varepsilon_0} \right) H'_{z1D} = \left(\varepsilon' + \frac{\Delta\varepsilon}{1 + j\omega\tau} + \frac{\sigma}{j\omega\varepsilon_0} \right) H_{z1D} \quad (10)$$

Hereinafter, the subscription “ $z1D$ ” is dropped for expression simplicity. The relationship between H' and H is then obtained from Equation (10). We multiply both sides of Equation (10) by $j\omega + (j\omega)^2\tau$, and implement the transformation $(j\omega)^n \leftrightarrow \partial^n/\partial t^n$ between frequency and time domain. This gives

$$\begin{aligned} & \frac{\sigma}{\varepsilon_0}H + \left(\varepsilon' + \Delta\varepsilon + \frac{\sigma\tau}{\varepsilon_0} \right) \frac{\partial H}{\partial t} + \varepsilon'\tau \frac{\partial^2 H}{\partial t^2} \\ &= \frac{\sigma}{\varepsilon_0}H' + \left(\varepsilon_\infty + \Delta\varepsilon + \frac{\sigma\tau}{\varepsilon_0} \right) \frac{\partial H'}{\partial t} + \varepsilon_\infty\tau \frac{\partial^2 H'}{\partial t^2} \end{aligned} \quad (11)$$

The discretization of Equation (11) in FDTD is of the following form:

$$H^{n+\frac{1}{2}} = R_0 \cdot H'^{n+\frac{1}{2}} + R_1 \cdot H'^{n-\frac{1}{2}} + R_2 \cdot H'^{n-\frac{3}{2}} - L_1 \cdot H^{n-\frac{1}{2}} - L_2 \cdot H^{n-\frac{3}{2}} \quad (12)$$

where

$$R_0 = \frac{2\beta_2 + \Delta t \cdot \beta_1}{2\alpha_2 + \Delta t \cdot \alpha_1}, \quad R_1 = \frac{-4\beta_2 + (\Delta t)^2 \cdot 2\beta_0}{2\alpha_2 + \Delta t \cdot \alpha_1}, \quad R_2 = \frac{2\beta_2 - \Delta t \cdot \beta_1}{2\alpha_2 + \Delta t \cdot \alpha_1},$$

$$L_1 = \frac{-4\alpha_2 + (\Delta t)^2 \cdot 2\alpha_0}{2\alpha_2 + \Delta t \cdot \alpha_1}, \quad L_2 = \frac{2\alpha_2 - \Delta t \cdot \alpha_1}{2\alpha_2 + \Delta t \cdot \alpha_1}, \quad \alpha_0 = \beta_0 = \frac{\sigma}{\varepsilon_0},$$

$$\alpha_1 = \varepsilon' + \Delta\varepsilon + \frac{\tau\sigma}{\varepsilon_0}, \quad \alpha_2 = \varepsilon'\tau, \quad \beta_1 = \varepsilon_\infty + \Delta\varepsilon + \frac{\tau\sigma}{\varepsilon_0}, \quad \beta_2 = \varepsilon_\infty\tau$$

The modified 1D Maxwell's equation top -wave in Debye dispersive layered media can be numerically computed by Equation (12) and the discretization form of (8) as commonly used in FDTD algorithm. It is worth pointing out that there is not any approximation, such as narrow band restriction, because of the θ in (9) being the incident angle other than the transmission angle in [4], required while the auxiliary variable H'_{z1D} in Equation (7) is implemented.

In 2D-FDTD, the simulation of plane wave along side TF-SF boundary at $i = i_r$ should especially treat the field component of

$H_z(i_r, j)$ and $E_y(i_r + 1/2, j)$ in expressions (2) and (4), they need the incident wave component of $E_y(i_r + 1/2, j)$ and $H_z(i_r, j)$ respectively, but the expressions (8) and (10) only contain H_z and E_x , there is no E_y . Fortunately, we note that (4) is the update equation about E_y , However which should work out the H_z along $i = i_r$ and $i = i_r + 1$. Then we should simulate twice by the expressions (8) and (10), the right TF-SF boundary is treated completely. The treatment to left boundary near $i = i_l$ is similarly.

3.2. CPML ABC for Modified 1D-FDTD

The modified 1D Maxwell's equation is used as the governing equation for incident wave in layered media along the side TF-SF, as discussed above. The Mur's ABC can be used to truncate the side TF-SF, AD or BC , as shown in Figure 1, providing the lowest layer medium is non-dispersive and lossless. While the dispersive and lossy media is of interest as considered in this paper, we implement the CPML ABC to truncate side TF-SF boundary.

Following the first and third equation of (8) and [6, 9], the Ampere's law in the CPML region is then expressed as

$$\begin{aligned} \varepsilon_0 \varepsilon_\infty \frac{\partial E_{x1D}}{\partial t} + \sigma E_{x1D} + J_{x1D} &= \frac{1}{\kappa_y} \frac{\partial H_{z1D}}{\partial y} + \zeta_y * \frac{\partial H_{z1D}}{\partial y} \\ \mu_0 \frac{\partial H'_{z1D}}{\partial t} &= \frac{1}{\kappa_y} \frac{\partial E_{x1D}}{\partial y} + \zeta_y * \frac{\partial E_{x1D}}{\partial y} \end{aligned} \quad (13)$$

The expression of κ_y and ζ_y in Equation (13) can be found in [6, 9]. The RC technique can be implemented to manipulate the convolution in (13) in FDTD computation, as reported by Luebbers [6, 10].

For simplicity in programming, the side TF-SF is extended till to the bottom of 2D-FDTD computation region, as shown in Figure 1. The thickness and parameters of CPML chosen in 1D and 2D FDTD are identical to each other.

3.3. Treatment of upper TF-SF Boundary in Free Space

Suppose $A'(i, j_u)$ is an arbitrary grid point on the upper TF-SF AB , as shown in Figure 2. Considering that the upper TF-SF boundary AB is parallel to the interface and located in free space, the incident waveform at point A' is the duplication of the waveform at corner A of upper TF-SF with a proper time delay $\Delta T_{AA'}$,

$$\Delta T_{AA'} = |AA''|/c_0 = (i_r - i) \cdot \Delta x \cdot \sin \theta / c_0 \quad (14)$$

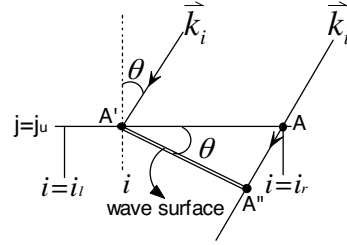


Figure 2. Incident wave along the upper TF-SF boundary.

where θ is the angle of incidence, c_0 the wave velocity in free space. If $\Delta T_{AA'}$ is not an integer multiple of Δt , say $\Delta T_{AA'} = (l + w) \Delta t$, where l is integer number and $0 < w < 1$, the linear interpolation scheme can be used as follows:

$$H_{z,inc}^n(i, j_u) = (1 - w) H_{inc}^l(i_r, j_u) + w H_{inc}^{l+1}(i_r, j_u) \quad (15)$$

in which (i_r, j_u) stands for the grid point at corner A .

3.4. Treatment of Lower TF-SF Boundary

Due to the incident wave on the lower TF-SF boundary is in fact the transmitted wave that is propagating outwards to the total field region, the incident waveform at a point on the lower TF-SF is also identical to the waveform at corner of lower TF-SF with a proper time delay, as discussed for the upper TF-SF, providing the lowest layer medium is non-dispersive and lossless. The time delay may be calculated by Equation (14) as well, except for θ representing the refracted angle and the wave velocity in lowest layer medium.

In the case of lowest layer medium being dispersive and lossy, we may extend the lower TF-SF boundary CD downwards into CPML, as shown in Figure 1. With this arrangement, it is not necessary to calculate the components of incident wave along the lower TF-SF any more.

4. EXAMPLES

4.1. Half-space Model

The galactophore tissue [11] is a simple half-space model. The lower layer medium is non-magnetism, dispersive and lossy, and upper is free space, their interface is located at $y = 0$. Debye medium in this example is characterized by a single pole, as shown in Equation (1)

where $\varepsilon_\infty = 7.0$, $\varepsilon_s = 10.0$, $\sigma = 0.15 \text{ S/m}$ and $\tau = 7.0 \times 10^{-12} \text{ s}$. In FDTD computation we take $\delta = 1.25 \times 10^{-4} \text{ m}$ and $\Delta t = 2.1 \times 10^{-13} \text{ s}$. The FDTD domain is $[-50: 50, -50: 50]$, outermost shell is 10 layers CPML, and TF region is $[-45: 45, -60: 45]$. The impinging Gaussian pulse [6] wave source is shown as

$$H_i(t) = \exp[-4\pi(t - t_0)^2/T^2] \quad (16)$$

where $\Delta t = \delta/2c_0$, the width of pulse is $T = 60\Delta t$, $t_0 = 0.8T$, and the incident angle $\theta = 30^\circ$.

The reflection waveform in time-domain at the node (45, 30) computed by modified 1D-FDTD is shown in Figure 3 by solid line. The result calculated by Fourier transform and analytical reflection coefficient [12, 13] is also displayed by dash line for comparison. They are in good agreement that validates our proposed scheme.

Figure 4 illustrates the distribution of magnetic field at different time steps along the side TF-SF AD as shown in Figure 1, which is computed by the modified 1D-FDTD. The Gaussian pulse is incident to the interface $y = 0$ from free space $y > 0$. The wave front arrives at and across the interface $y = 0$ at $t = 120\Delta t$ and $170\Delta t$, respectively, as shown in Figure 4. The reflected and transmitted waves are then propagating in different direction and apart from each other at $t = 220\Delta t$, as shown in Figure 4. It can also be seen from the waveform at $500\Delta t$ that the absorption boundary CPML works well for modified 1D-FDTD.

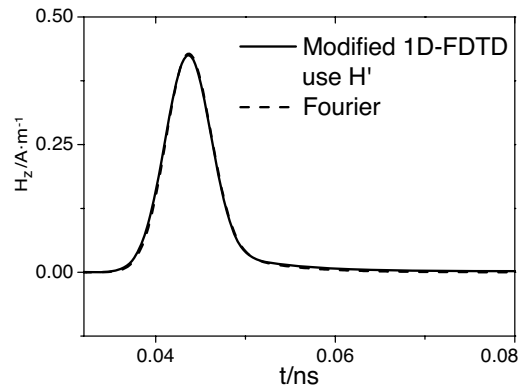


Figure 3. Waveform in time-domain at node (45, 30).

4.2. Multi-layer Model

A four layer model consists of free space, dry soil, water and wet soil from top to bottom. The thickness and constitutive parameters in

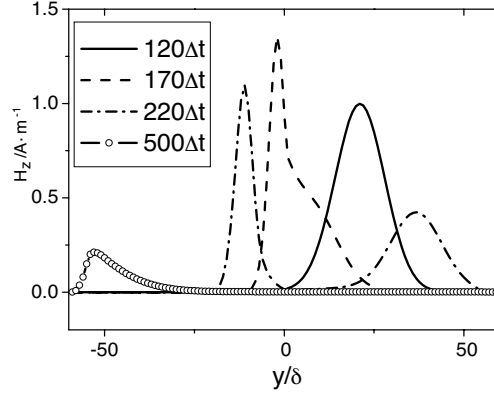


Figure 4. Distribution of magnetic field along side TF-SF AD at different time steps.

computation are given in Table 1. In the 2D-FDTD simulation we take $\delta = 0.2$ cm, and FDTD region is within $[-200: 200, -500: 500]$, surrounded by 10 layer CPML. The TF region is $[-195: 195, -510: 495]$, in which the interface between dry soil and water is located at $y = 0$. The Gaussian pulse as in Equation (16) of $\Delta t = \delta/2c_0$, $T = 220\Delta t$ and $t_0 = 0.8T$ is impinging from free space with the incident angle of $\theta = 20^\circ$.

Table 1. Parameters for four layer media.

Media	ϵ_s	ϵ_∞	σ (S/m)	τ (s)	Thickness (m)
Free space	1.0	1.0	0.0	-----	-----
Dry soil	7.73	7.73	0.0	-----	0.6
Water	1.8	81.0	43.43	9.4×10^{-12}	0.4
Wet soil	7.73	7.73	0.273	-----	-----

The waveform of magnetic field H_z at observation point (0.39 m, 0.9 m) calculated by modified 1D-FDTD is plotted in Figure 5. It can be observed that the first wave crest (A) is the incident Gaussian pulse, followed by the wave (B) reflected from the upper interface between free space and dry soil. The crest (C) in figure comes from the reflection from the lower interface between dry and water.

Note that the time interval between successive crests after (C) is about 11.1 ns. This can be explained as follows: the wave speed in dry soil is $c = c_0/\sqrt{7.73}$, where $c_0 = 3.0 \times 10^8$ m/s and the vertical speed

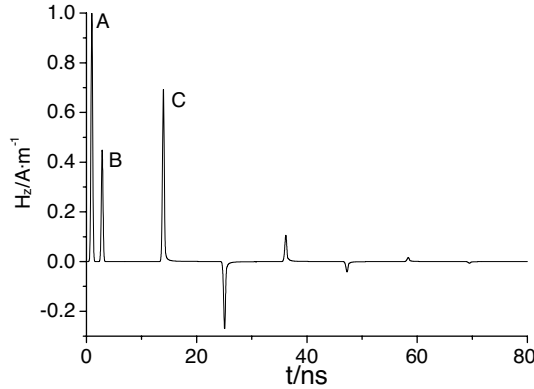


Figure 5. Hz waveform simulated by modified 1D-FDTD at the point (0.39 m, 0.9 m).

is $c' = c/\cos\theta_d''$. The refraction angle in dry soil θ_d'' can be derived by $\sin\theta_d'' = \sin\theta/\sqrt{7.73}$. Therefore the round-trip time in dry soil layer is $t_{round} = 2 \times 0.6/c' \approx 11.0$ ns. Furthermore, the electromagnetic wave propagating in water layer is almost dissipated for the high-loss of water. Thus the affect of water and wet soil layers to waveform in Figure 5 can hardly be observed.

Figure 6 gives the snapshot at different time steps, where wave crests are mainly located (a) near the interface between free space and dry soil at $700\Delta t$; (b) within the dry soil layer at $2000\Delta t$; (c) and (d) near the interface between dry soil and water at $2300\Delta t$ and $3000\Delta t$, respectively. The dash lines in the figure indicate the interfaces between different media. It is observed that the refraction angle in dry soil is $\theta_d'' \approx 7.07^\circ$ that is in good agreement with the theoretical calculation, and the width of pulse in dry soil becomes much narrower than that in free space, because of the slower wave velocity in dry soil.

It can also be seen from (c) and (d) in Figure 6, the electromagnetic wave at the interface between dry soil and water is reflected strongly because water is high-lossy medium. On the other hand, the refracted wave in water decays rapidly. The relative refractive index of water with respect to dry soil is approximate equal to 3.24 for low frequency; the refraction angle is $\theta_w'' = \sin 20^\circ/\sqrt{81.0} = \sin\theta_d''/3.24 \approx 2.2^\circ$ in water layer that is approximately equal to 0° .

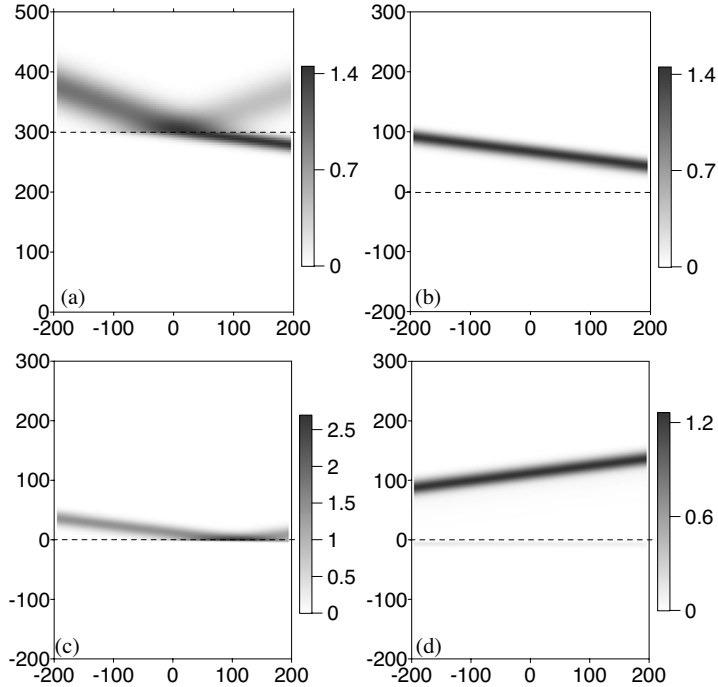


Figure 6. Snapshot to four layers model at different time. (a) ~ (d) are the component of magnetic field H_z at 700, 2000, 2300 and 3000 time step, respectively.

4.3. Scattering Problem

The analysis of EM scattering problem using FDTD is an interesting research area [14–22]. Suppose the galactophore tissue is of thickness 0.01 m, in which there is cancerization [11] at depth of 0.25 cm with radius 0.075 cm. Assume the top and bottom layers are both free space. Constitutive parameters of the galactophore tissue are the same as in Section 4.1, and that of the carcinosarcoma are $\epsilon_\infty = 3.99$, $\epsilon_s = 54.0$, $\sigma = 0.7 \text{ S/m}$ and $\tau = 7.0 \times 10^{-12} \text{ s}$. We take $\delta = 2.5 \times 10^{-4} \text{ m}$ in FDTD and $\Delta t = 4.17 \times 10^{-13} \text{ s}$. The FDTD region and the incident wave are also the same as in Section 4.1 except for $T = 60\Delta t$.

Figure 7 gives the snapshot at different time. The interfaces between the free space and the galactophore tissue are located at $y = 20\delta$ and -20δ ; the dash lines and circles in the figure show the interfaces between media and the carcinosarcoma, respectively. The scattered fields at node $(0, 47)$ by the layered galactophore tissue with

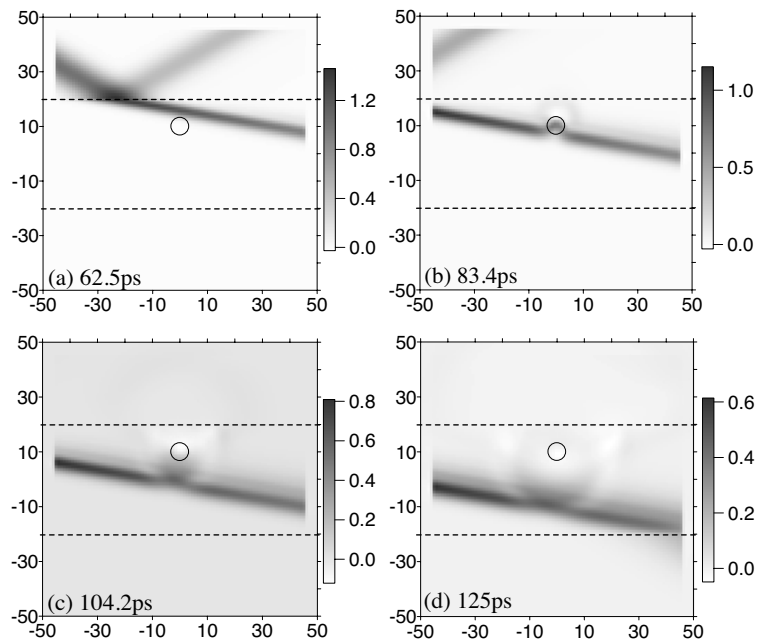


Figure 7. Snapshot to the galactophore tissue with carcinosarcoma.

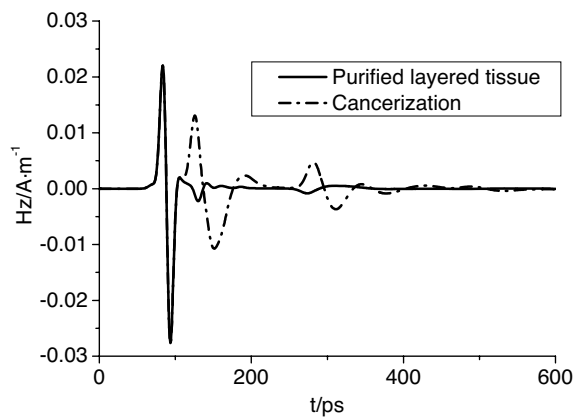


Figure 8. Scattering field received at node (0, 47) by the purified layered galactophore tissue and that with carcinosarcoma.

and without carcinosarcoma are depicted in Figure 8, respectively, which may help the analysis of this phenomenon.

5. CONCLUSION

The analysis of scattering problem in dispersive and lossy layered medium half-space by FDTD is considered in this paper. To impose the obliquely incident plane wave into the total field region we implement a non-closed TF-SF scheme, in which a new modified 1D-FDTD to p -wave is proposed. The lower TF-SF is set down to the CPML so that the TF-SF boundary is, in fact, of Π -shape and not closed. Computation examples are compared with the analytical solution and Fourier transform result, which validate the feasibility of proposed scheme.

ACKNOWLEDGMENT

This work is supported by the National Natural Science Foundation of China (Grant No. 40674060).

REFERENCES

1. Yee, K. S., "Numerical solution of initial boundary value problems involving Maxwell equations in isotropic media," *IEEE Trans. on Antennas Propagation*, Vol. 14, No. 3, 302–307, 1966.
2. Wong, P. B., G. L. Tyler, J. E. Baron, et al., "A three-wave FDTD approach to surface scattering with applications to remote sensing of geophysical surface," *IEEE Trans. on Antennas Propagation*, Vol. 44, No. 4, 504–513, 1996.
3. Yun, Y., B. Chen, D.-G. Fang, et al., "A new 2-D FDTD method applied to scattering by infinite objects with oblique incidence," *IEEE Trans. Electromagn. Compat.*, Vol. 47, No. 4, 756–62, 2005.
4. Winton, S. C., P. Kosmas, and C. M. Rappaport, "FDTD simulation of TE and TM plane waves at nonzero incidence in arbitrary layered media," *IEEE Trans. Antennas Propagat.*, Vol. 53, No. 5, 1721–1728, 2005.
5. Capoglu, I. R. and G. S. Smith, "A total-field/scattered-field plane-wave source for the FDTD analysis of layered media," *IEEE Trans. Antennas Propag.*, Vol. 56, No. 1, 158–169, 2008.
6. Taflove, A. and S. C. Hagness, *Computational Electrodynamics: The Finite-Difference Time-Domain Method*, Artech House, Norwood, MA, 2005.

7. Oguz, U. and L. Gurel, "Interpolation techniques to improve the accuracy of the plane wave excitations in the finite difference time domain method," *Radio Science*, Vol. 32, No. 6, 2189–2199, 1997.
8. Oguz, U., L. Gurel, and O. Arıkan, "An efficient and accurate technique for the incident-wave excitations in the FDTD method," *IEEE Trans. Microwave Theory Tech.*, Vol. 46, No. 6, 869–882, 1998.
9. Roden, J. A. and S. D. Gedney, "Convolutional PML (CPML): An efficient FDTD implementation of CFS-PML for arbitrary media," *Microwave Opt. Tech. Lett.*, Vol. 27, No. 12, 334–339, 2000.
10. Luebbers, R. J., F. P. Hunsberger, K. S. Kunz, et al., "A frequency-dependent finite-difference time-domain formulation for dispersive materials," *IEEE Trans. on EMC*, Vol. 32, No. 3, 222–227, 1990.
11. Converse, M., E. J. Bond, S. C. Hagness, et al., "Ultrawide-band microwave space-time beam forming for hyperthermia treatment of breast cancer: A computational feasibility study," *IEEE Trans. Microwave Theory Tech.*, Vol. 52, No. 8, 1876–1889, 2004.
12. Kong, J. A., *Electromagnetic Wave Theory (6)*, Higher Education Press, Beijing, 2002.
13. Rui, P.-L. and R.-S. Chen, "Implicitly restarted gamres fast Fourier transform method for electromagnetic scattering," *Journal of Electromagnetic Waves and Applications*, Vol. 21, No. 7, 973–986, 2007.
14. Zainud-Deen, S. H., A. Z. Botros, and M. S. Ibrahim, "Scattering from bodies coated with metamaterial using FDTD method," *Progress In Electromagnetics Research B*, Vol. 2, 279–290, 2008.
15. Hu, X.-J. and D.-B. Ge, "Study on conformal FDTD for electromagnetic scattering by targets with thin coating," *Progress In Electromagnetics Research*, PIER 79, 305–319, 2008.
16. Yang, L.-X., D.-B. Ge, and B. Wei, "FDTD/TDPO hybrid approach for analysis of EM scattering of combinative objects," *Progress In Electromagnetics Research*, PIER 76, 275–284, 2007.
17. Uduwawala, D., "Modeling and investigattion of planar parabolic dipoles for GPR application: A comparison with bow-tie using FDTD," *Journal of ElectroMagnetic Waves and Applications*, Vol. 20, No. 2, 227–236, 2006.
18. Tan, K.-B., L. Li, and C.-H. Liang, "Canonical analysis for disspersive electromagnetic medium," *Journal of Electromagnetic Waves and Applications*, Vol. 21, No. 11, 1499–1505, 2007.
19. Sukharevsky, O. I. and V. A. Vasilets, "Scattering of reflector an-

- tenna with conic dielectric radome,” *Progress In Electromagnetics Research B*, Vol. 4, 159–169, 2008.
20. Wang, M.-J., Z.-S. Wu, and Y.-L. Li, “Investigation on the scattering characteristics of Gaussian beam from two dimensional dielectric rough surfaces based on the Kirchhoff approximation,” *Progress In Electromagnetics Research B*, Vol. 4, 223–235, 2008.
 21. Abd-El-Ranouf, H. E. and R. Mittra, “Scattering analysis of dielectric coated cones,” *Journal of Electromagnetic Waves and Applications*, Vol. 21, No. 13, 1857–1871, 2007.
 22. Wang, M. Y., J. Xu, J. Wu, et al., “FDTD study on scattering of metallic column covered by double-negative metamaterial,” *Journal of Electromagnetic Waves and Applications*, Vol. 21, No. 14, 1905–1914, 2007.